Talanta 94 (2012) 50–57

Contents lists available at SciVerse ScienceDirect

Talanta

journal homepage: www.elsevier.com/locate/talanta

Determination of metal impurities in advanced lead zirconate titanate ceramics by axial view mode inductively coupled plasma optical emission spectrometry

M.E. Villanueva Tagle[a], M.T. Larrea Marín[b], O. Martin Gavilán[c], M.D. Durruthy Rodríguez[d], F. Calderón Piñar[e], M.S. Pomares Alfonso[e,*]

[a] Facultad de Química, Universidad de La Habana, 10400 La Habana, Cuba
[b] Centro Nacional de Investigaciones Metalúrgicas (CSIC), 28040 Madrid, Spain
[c] Centro de Espectrometría Atómica, Universidad Complutense de Madrid, 28040 Madrid, Spain
[d] Instituto de Cibernética, Matemática y Física, CITMA, 10400 La Habana, Cuba
[e] Instituto de Ciencia y Tecnología de Materiales, Universidad de La Habana, 10400 La Habana, Cuba

ARTICLE INFO

Article history:
Received 14 November 2011
Received in revised form 17 February 2012
Accepted 22 February 2012
Available online 1 March 2012

Keywords:
PZT ceramic impurities
Axial view mode ICP-OES
Matrix effect
Signal-to-background ratio
Line intensity

ABSTRACT

An inductively coupled plasma optical emission spectrometry quantification method for the determination of Al, Ca, Cr Cu, Fe, Mn, Mg, Ni, Zn, Ba, K, In and Co in lead zirconate-titanate (PZT) ceramics, modified with strontium and chromium, was developed. Total digestion of ceramics was achieved with a HNO_3, H_2O_2 and HF (ac) mixture by using a microwave furnace. The sensitivity of the net signal intensity respect to radiofrequency power (P) and nebulizer argon flow (F_N) variations was strongly dependent of the total excitation energy of line (TEE). For lines with TEE near metastable atoms and ions of argon, an increment of the sensitivities to P and F_N variation was observed. At robust plasma conditions the matrix effect was reduced for all matrices and analytes considered. The precision of analysis ranged from 3 to 13%, whereas the analytes recoveries in the spiked samples varied, mostly, from 90 to 110%. The detection limits of studied elements were from 0.004 to 10 mg kg^{-1}.

1. Introduction

Lead zirconate-titanate ceramics (PZT) are widely employed in electronic devices such as vibration or temperature sensors, and ultrasound generators due to piezoelectric properties. These properties can be improved by keeping a rigorous control of the concentration of elements intentionally added in order to modify the stoichiometry of ceramics and of traces eventually incorporated to the material during the synthesis process. Impurities such as Al, Ba, Ca, Li, Mg, Cu, Fe and Na, among others, can affect, significantly, the microstructure of the final products; and, consequently, the ferroelectric-piezoelectric properties and quality of the PZT ceramics [1,2].

A variety of techniques, including X-ray fluorescence [3] and Transmission and Scanning Electron Microscopy [4,5] have been applied for determining the stoichiometry of elements in thin layers, layered system and bulk ceramic materials. Although these techniques allow the analysis of solid materials directly, sometimes they are not sufficiently sensitive for detecting the traces present as impurities. An additional drawback of those techniques is the lack of PZT solid standards for calibration [6]. Inductively coupled plasma optical emission spectrometry (ICP-OES), despite the necessity to decompose the sample, is sensitive enough for the determination of traces in a broad type of samples with high accuracy and precision [7]. Another great advantage of the technique is that it allows the simultaneous determination of major, minor and trace elements. On the other hand, the calibration can be performed with the analyte in solution. Interestingly, the ICP-OES technique has been little used for investigating the impurities presence in ceramic materials [6,8–10].

As known [11,12], the axially viewing observation mode is recommended for the improvement of the detection limits. However, special attention should be, then, devoted to the matrix effect (ME) because it can be larger in axial than in radial view mode [11,13]. Thus, the accuracy of analysis can be, additionally, more deteriorated in axial than in view mode [14]. Therefore, the principal aim of the present work was to develop a rigorously based analytical method for the reliable and accurate determination of Al, Ca, Cu, Fe, Mn, Mg, Ni, Zn, Ba, K, In, Co impurities, and doped Cr in PZT ceramics modified with strontium and chromium by axially viewing ICP-OES. Special attention will be dedicated to the selection of the radiofrequency power (P) and nebulizer argon flow (F_N) operating parameters. In addition, a study of the ME behaviour for lines with a wide interval of total energy excitation (TEE) shall be made.

* Corresponding author.
E-mail address: mpomares@imre.oc.uh.cu (M.S. Pomares Alfonso).

0039-9140/$ – see front matter © 2012 Elsevier B.V. All rights reserved.
doi:10.1016/j.talanta.2012.02.045

Table 1
SPECTRO ARCOS optical emission spectrometer operating parameters.

Parameter	Value
Injector ceramic tube internal diameter (mm)	2
Spray chamber type	Cyclonic
Nebulizer type	Lichte model
Plasma power (kW)	1.4[a]
Auxiliary argon flow rate (L min^{-1})	0.6
Nebulizer argon flow rate (L min^{-1})	0.8[a]
Plasma viewing mode	Axial
Background correction	2 points per peak

[a]Selected for the final analysis of ceramic samples.

2. Materials and methods

2.1. Instrumentation

A SPECTROARCOS EQ 3700 (Spectro, Germany) ICP-OES spectrometer was used. The experimental conditions finally used for the analysis are resumed in Table 1.

2.2. Reagent, solutions and samples

Analytical grade 65% (m/m) HNO_3, 37% (m/m) HCl, 48% (m/m) HF, and 30% (m/m) H_2O_2 all from Merck were used. Deionised water (resistivity of 18.2 MΩ cm), purified by a Milli-Q system (from Millipore) was employed for calibration solutions and samples preparation. Calibration solutions were prepared by serial dilution of 1000 mg L^{-1} (Titrisol®, Merck) mono element stock solutions. Two groups of calibration solutions were prepared; one for major elements and another for traces. The first group included Pb, Zr, Ti and Sr from 5 to 50 mg L^{-1} of concentrations. The second group included Al, Ca, Cu, Cr, Fe, Mn, Mg, Ni, Zn, Ba, K, In and Co at concentrations in the range of 0.1 to 10.0 mg L^{-1}. All solutions were prepared in 5% (v/v) HNO_3.

The PZT ceramics of general formula $Pb_{0.95}Sr_{0.05}(Zr_{1-x}Ti_x)_{1-y}Cr_yO_{3-y/2}$, considered in this work, were produced at the Instituto de Cibernética, Matemática y Física (ICIMAF), Cuba, according to the method previously reported [5]. Oxides and carbonates of analytical grade, 98% $PbCO_3$ (BDH, England), 99% ZrO_2 (Merck, Germany), 99% TiO_2 (Riedel de Haen, Germany), spectrally pure $SrCO_3$ (Fluka AG, Germany) were used for the PZT ceramic synthesis. Three sets of ceramics with different contents of Ti and Zr (Zr/Ti molar ratio = 53/47; 60/40 and 80/20) were prepared. Keeping a constant Zr/Ti molar ratio in each set, six different ceramic samples were synthesized with the addition of different concentrations of Cr. The coefficient "*y*" in the general formula mentioned above were 0.0; 0.1; 0.2; 0.3; 0.4 and 0.5, respectively. Synthesized ceramics were pulverized and homogenized in agate mortar before the decomposition in the laboratory.

2.3. Sample decomposition

Two different reported [15,16] microwave-assisted procedures, Procedure I and II, graphically resumed in Fig. 1, were evaluated on a Zr/Ti = 60/40 ceramic without Cr, coefficient $y = 0.0$, taken as example. The two microwave digestion programs (Program No 1 and Program No 2), employed in both decomposition procedures I and II, are shown in Table 2. Three replicate of samples were digested by each procedure and further analyzed at routine operating conditions ($P = 1.4$ kW and $F_N = 1$ L min^{-1}. The average concentrations of determined analytes were statistically compared for a confidence level of 95%. For the final determinations, PZT ceramic samples were decomposed in triplicate according to the Procedure I. The solutions obtained were diluted 1:500 for Sr and 1:1000 for Ti, Pb and Zr major element determinations.

2.4. Spectral interference and matrix effect

Two or more lines of the thirteen traces to be determined in PZT ceramics were selected from the recommended database lines of the spectrometer software. The possible spectral interferences were investigated over a total of thirty-eight spectral lines showed in Table 3 by comparing the emission spectrum of the solution 1.2 (Table 4) of the traces plus Ti, Zr, Pb and Sr major elements with the corresponding spectrum of the matrix blank (solution 2.2). The major element composition of both solutions simulated the composition of the diluted PZT ceramics with intermediate molar ratio Zr/Ti = 60/40.

ME on the thirty-eight analytical lines of Al, Ca, Cu, Cr, Fe, Mn, Mg, Ni, Zn, Ba, K, In and Co was calculated, in percentage, according to Eq. (1)

$$\mathrm{ME}\,(\%) = \left[\frac{I_1 - I_2}{I_3 - I_4} - 1\right] \times 100 \quad (1)$$

where, I_1 is the trace emission intensity in the presence of major elements, measured in the type 1 solutions of Table 4. The three different type 1 solutions 1.1, 1.2 and 1.3, simulated the three diluted ceramics, considered in this work, with molar ratio Zr/Ti of 20/80 (matrix I), 60/40 (matrix II) and 80/20 (matrix III), respectively. I_2 was measured in the three different type 2 matrix blank solutions 2.1, 2.2 and 2.3. I_3 was measured in the absence of major elements (solutions 3.1, 3.2 and 3.3) and I_4 is the trace emission intensity measured in the type 4 solution, which is the blank of the type 3 solution. Three replicates of each solution were measured at two different times during a working session; hence, the calculated EM was the mean of six replicates.

2.5. Operating parameters

The radiofrequency power (P) and nebulizer argon flow (F_N) were optimized for the determination of traces (the doped Cr and impurities). The net signal intensity (I_N) and signal-to-background ratio (SBR) were calculated as the average of three measurement replicates of a solution containing 5 mg L^{-1} of Al, Ca, Cu, Cr, Fe, Mn, Mg, Ni, Zn, Ba, K, In and Co in the presence of the sample matrix II (Zr/Ti = 60/40). The concentrations of Pb, Zr, Ti and Sr in sample matrix II were 3000, 850, 300 and 72 mg L^{-1} respectively. The I (MgII 280.270 nm)/I (MgI 285.213 nm) ratio (MgII/MgI) was measured in the presence and absence of the sample matrix as an indicator of the plasma robustness.

2.6. Method evaluation

Precision was evaluated as the relative standard deviation (RSD), whereas nine replicates of the ceramic sample solution were measured. Since there was no appropriate certified reference material commercially available for PZT ceramics, the accuracy of the developed analytical methodology was evaluated by using the added-recovered method. Three replicates of the ceramic sample with molar ratio Zr/Ti = 60/40, taken as example, were spiked with the investigated elements and then submitted to decomposition according to Procedure I. Three replicates of the sample without analyte addition were analyzed in parallel as well as a triplicate of the blank. The analyte in each replicate was measured three times by ICP-OES, at different moments in a work session. Then, the average recovered concentration was expressed as percentage respect to the added concentration.

The limits of detection (LODs) of Cr and impurities (Al, Ca, Cu, Fe, Mn, Mg, Ni, Zn, Ba, K, In and Co) were determined by interpolating in each element calibration curve the element line intensity at limit of detection (I_{LOD}) calculated as $I_{LOD} = b + 3s$, where "*b*" is the average background intensity of the analyte measured in 10 replicates of

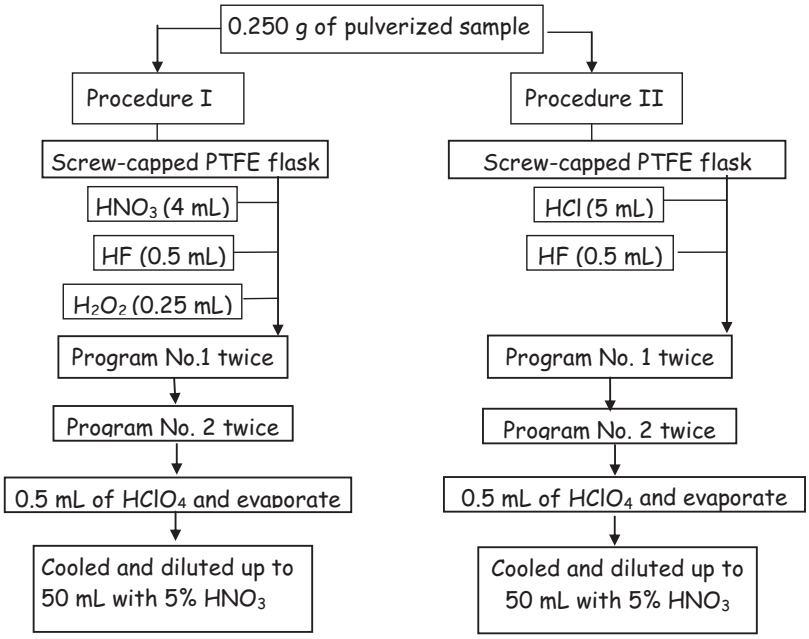

Fig. 1. Resume of the sample decomposition procedures studied.

Table 2
Microwave-assisted acid-digestion heating programs.

Program	Parameter	Step 1	Step 2	Step 3	Step 4	Step 5	Step 6	Step 7	Step 8
1	Power (W)	250	0	200	0	–	–	–	–
	Time (min)	10	5	5	2	–	–	–	–
2	Power (W)	250	0	400	0	600	0	2	5
	Time (min)	10	5	4	5	5	5	200	0

Table 3
Emission lines studied with the corresponding excitation energy for atomic (I) and total excitation energy (excitation plus ionization energy) for the ionic (II) lines.

Element	Energy (eV)	Element	Energy (eV)	Element	Energy (eV)
K I 766.491[a]	1.62	Al I 167.078	5.98	Cr II 205.618	12.8
Li I 670.780	1.85	Cr II 283.563[a]	6.76	Cr II 267.716	12.95
Na I 588.915	2.10	Mn II 259.373	7.43	Fe II 238.204	13.11
Na I 589.592	2.10	Ba II 455.404[a]	7.93	Ca II 317.933	13.16
Al I 396.152[a]	3.14	Ca II 393.366[a]	9.26	Co II 238.892	13.49
Cu I 327.396	3.79	In II 230.609	11.16	Co II 228.686[a]	13.72
Cu I 324.754[a]	3.82	Ba II 230.424	11.2	Co II 230.786	13.75
In I 325.609[a]	4.08	Ba II 233.527	11.22	Ni II 221.648[a]	14.27
Ni I 300.249	4.15	Mg II 280.270	12.07	Ni II 231.604	14.27
Mg I 285.213	4.35	Mg II 279.553[a]	12.08	Cd II 226.502	14.47
Li I 460.289	5.39	Mn II 260.569[a]	12.19	Cd II 214.438	14.77
Cd I 228.802	5.42	Mn II 257.611	12.25	Zn II 206.200	15.41
Zn I 213.856[a]	5.80	Fe II 259.941[a]	12.67	Zn II 202.613	15.51

[a] Lines employed for the final analysis of ceramic samples.

Table 4
Solutions prepared for the study of spectral and matrix interferences.

Solution type	Concentration of major elements ($mg\,L^{-1}$)				Concentration of the traces ($mg\,L^{-1}$)	Concentration of HNO_3 (%, v/v)
	Pb	Zr	Ti	Sr		
1.1	3000	850	300	72	10[a]	5
1.2	3220	298	626	72	50	5
1.3	2950	1100	144	66	50	5
2.1	3000	850	300	72	–	5
2.2	3220	298	626	72	–	5
2.3	2950	1100	144	66	–	5
3.1	–	–	–	–	10[a]	5
3.2	–	–	–	–	50	5
3.3	–	–	–	–	50	5
4	–	–	–	–	–	5

[a] Except Co, Zn and Ca at $30\,mg\,L^{-1}$.

Table 5
Decomposition procedures comparison.

Element	Average concentration ± confidence interval[a] (%, m/m)		Stoichiometric concentrations
	Procedure I ($HNO_3 + H_2O_2 + HF$)	Procedure II ($HCl + HF$)	
Zr	18.5 ± 0.2	18 ± 2	16.9
Pb	60 ± 1	24 ± 2	61
Ti	6.17 ± 0.05	6 ± 1	5.92
Sr	1.44 ± 0.01	1.1 ± 0.4	1.35

[a] $n = 3$, $\alpha = 0.05$. This experiment was performed at routine operating conditions used in the laboratory (nebulizer argon flow rate of 1 L min^{-1} and plasma power of 1.4 kW).

digestion blank solution, and "s" is the standard deviation of blanks concerning the replicates.

3. Results and discussion

3.1. Method development

The selection of the sample decomposition procedure was made by comparing the Pb, Zr, Ti and Sr expected stoichiometric concentrations with the concentrations experimentally found. As can be seen in Table 5, concentrations of Zr, Ti and Sr obtained by Procedure II were in good agreement, within the experimental error, with the concentrations values expected. In contrast, for Pb a large difference (~40%) between expected and found concentrations was observed. The precipitation of a part of the total Pb present in the solution, as a consequence of the insoluble $PbCl_2$ formation in an excess of HCl, could be a reasonable explanation for the Pb low concentration (24%). This relatively high amount of non dissolved Pb could influence on a poor extraction of the impurities to be quantified. Therefore, the Procedure II was discarded. In addition, less reproducible results for the rest of the elements were also obtained with this digestion procedure. On the other hand, the concentration of Pb obtained by the Procedure I matched strictly, within the experimental error, with the stoichiometric concentration; whereas concentration of Zr, Ti and Sr were lightly lower (between 4 and 9%) than expected. Therefore, we decided to select the Procedure I, which provided, in general, the best major element concentrations.

Spectral interferences were observed on Cu 224.700 nm and Cr 283.563 nm by Pb 224.689 nm, and Ti 283,562 nm lines, respectively; and on Al 309.271 nm by OH^- emission molecular band. The remaining spectral lines, shown in Table 3, were free from spectral interferences.

A systematic study of P and F_N influence on I_N of the thirty eight analytical lines of impurities Al, Ca, Cu, Cr, Fe, Mn, Mg, Ni, Zn, Ba, K, In and Co in presence of the sample matrix was carried out. A solution, simulating the intermediate matrix content (Zr/Ti = 60/40) of the diluted ceramics was used. Firstly, I_N *vs.* P and I_N *vs.* F_N relationships were experimentally obtained for each of the thirty-eight analytical lines. For a more detailed study, a first polynomial function were adjusted to I_N *vs.* P and I_N *vs.* F_N relationships for each analytical line, and the corresponding slopes were calculated. Thus, slopes represent the sensitivity of the net signal intensity respect to the variation of the corresponding operating parameter, P or F_N. Thereafter, the slopes of I_N *vs.* P and I_N *vs.* F_N relationships, as a function of TEE of the analytical lines were investigated (Fig. 2).

As previous reported for radial view mode ICP-OES [7], the I_N increased (slope > 0) with the increment of P for the most of lines studied (Fig. 2a). However, the I_N sensitivity respect to the P variation depended of the TEE of the line in a complex way. Interestingly, Ca II 393.366 nm, MgII 280.270 nm, MgII 279.573 nm and MnII 260.569 nm with TEE equal to 9.26 eV, 12.07 eV, 12.08 eV and 12.19 eV, respectively, were among the most sensitive of the all lines studied. In Fig. 2a, just two lines, MgII 280.270 nm and MnII 260.569 nm lines, were identified for clarity purposes; while the slopes of CaII 393.366 nm and MgII 279.573 nm lines were not visualized because they were higher than the maximum of the "*y*" axe. The preferential increment of sensitivity observed, may be explained as an over excitation of those lines provided by a Penning Reaction [17,18], which could act selectively on the specific spectral emission lines with TEE near to the excitation energy (11.548–11.723 eV) of the metastable atoms of Ar. A second group of lines (see the slope values surrounded by a circle in Fig. 2a) with TEE near the first ionization energy (15.6 eV) of Ar atoms, showed also a preferential increment of I_N with P variation. The explanation of this specific behaviour could be an over excitation of those lines by the Charge Transference mechanism, observed in radial [19] and axial [20] view observation mode between analyte atoms and Ar ions. Lastly, lines with TEE ~2 eV and TEE ~8 eV, showed a slightly higher increment of the I_N sensitivity respect to the P variation in comparison with the rest of lines in the 2–8 eV energy interval. For instance, LiI 670.780 nm, NaI 589.592 nm and NaI 588.915 nm lines with lower TEE, from 1.85 to 2.10 eV; and MnII 259.373 nm and BaII 455.404 nm with higher TEE, around 7–8 eV. This complex behaviour between the power variation sensitivity of intensities and the TEE of lines, observed in axial view mode for the three group of lines above mentioned was not reported previously in radial view mode.

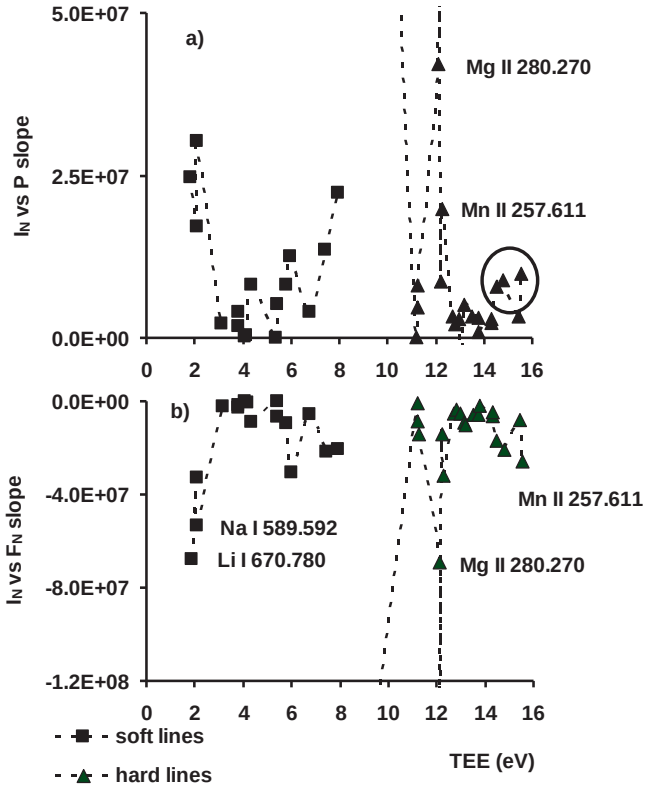

Fig. 2. Dependence of the net signal intensity (I_N) *vs.* radiofrequency power (P) applied (a) and I_N *vs.* nebulizer flow rate (F_N); (b) relationship slopes with the total excitation energy (TEE) of the line.

The higher sensitivity of I_N respect to the F_N variation (Fig. 2b) was also observed, approximately, for the same three group of lines; which showed a high power variation sensitivity in Fig. 2a, *i.e.*, lines with extreme TEE in the 2–8 eV interval, lines with TEE around metastable atom Ar energy and lines with TEE around first ionization energy of Ar atoms. However, the effect was opposed, *i.e.*, the I_N decreased (slope <0) with the increment of F_N. The reduction of

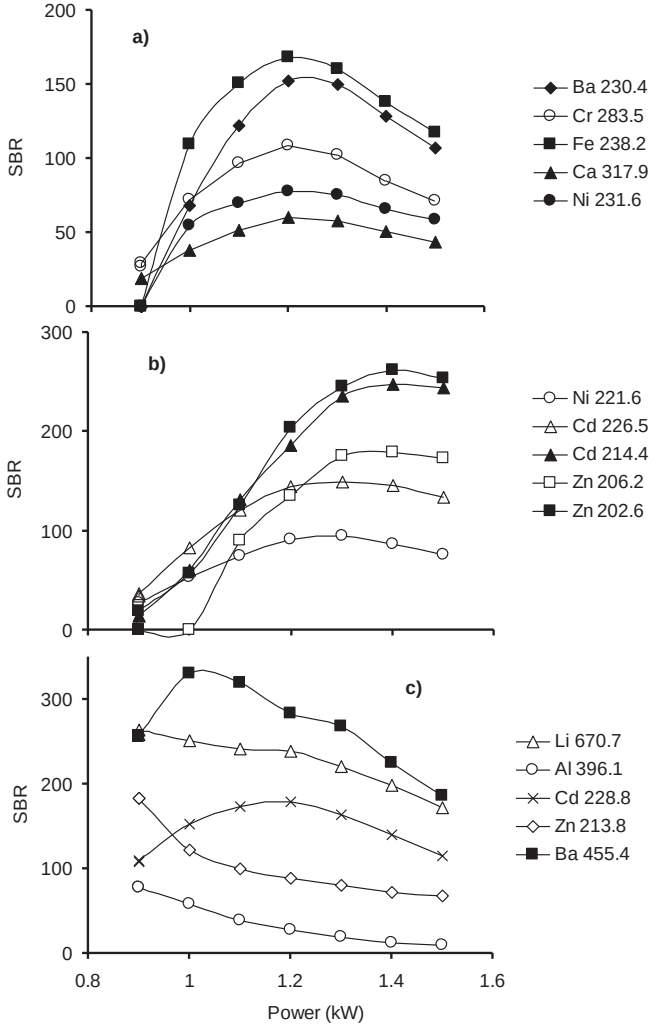

Fig. 3. Radiofrequency power (P) influence on signal-to-background ratio (SBR) of hard (a and b) and soft (c) lines. This experiment was performed at argon nebulizer flow of 0.95 L min^{-1}.

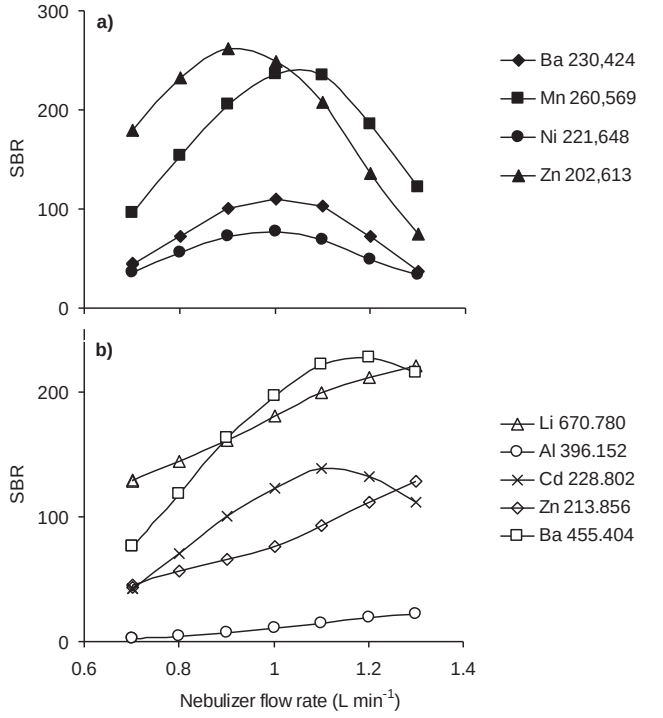

Fig. 4. Nebulizer flow rate (F_N) influence on signal-to-background ratio (SBR) of hard (a) and soft (b) lines. This experiment was performed at radiofrequency power of 1.5 kW.

the line net intensity could be explained by the decrease of the residence time of atoms in the plasma excitation zone; when F_N was incremented. Then, the residence time diminution did not favour the excitation of lines. In the same way, the selective excitation of atoms by Penning Reaction and Charge Transference mechanisms was not favoured; which, in turn, decreased the probability of the energy transference among particles in the plasma.

SBR influences directly on the ICP-OES limit of detection (LOD) [21]. A systematic study of the variation of the SBR with P and F_N was performed for analytical lines under study (Figs. 3 and 4). According to the univariate approach used in the present study, one of the two studied variables, P or F_N, was fixed at a constant value; while the second one was varied. During the study of the influence of the radiofrequency power, the argon nebulizer flow was fixed, approximately, at an intermediate value (F_N = 0.95 L min^{-1}) among all possible ones within the variation interval available in the instrument (0.7–1.3 L mim^{-1}). However, the study of influence of F_N was performed at P = 1.5 kW, higher than the intermediate value of 1.1 kW, because otherwise the plasma became unstable for higher values of F_N and the scope of the study would be seriously reduced. This way, it was possible to perform the study over the entire variation interval of nebulizer flow. For clarity purposes, just a representative selection of the results of all the studied lines was included. Thus, by fixing F_N at 0.95 L min^{-1}, maximum SBR (SBR_M) of lines with TEE between 10 and 16 eV was observed, generally, at P in the interval of ~1.2–1.4 kW (Fig. 3a and b). It should be noted that, SBR_M shifted toward higher P, around 1.3–1.4 kW, for lines with TEE higher than 14.27 eV (Fig. 3b). For the most of lines with TEE between 2 and 8 eV (Fig. 3c), SBR_M was reached at lower P (~0.9 kW), excepting Cd 228.802 nm, Na 589.592 nm and Ba 455.404 nm lines with SBR_M at a little higher P of ~1.0–1.2 kW.

The variation of SBR with F_N, by fixing P at 1.5 kW, is shown in Fig. 4. For lines (Fig. 4a), SBR_M was reached at F_N around 1.0–1.1 L min^{-1}, except for lines with TEE higher (see, for example, the Zn II 202.613 nm line with TEE = 15.51 eV in Fig. 4a), for which SBR_M was slightly displaced to a lower F_N of 0.9 L min^{-1}. On the contrary, SBR of lines in the 2–8 eV interval continuously increased with the increment of F_N (see, for example, LiI 670.780 nm line in Fig. 4b) or reached SBR_M at higher F_N of 1.2 L min^{-1} (see, for example, BaI 455.404 nm line in Fig. 4b).

In resume, the SBR *vs.* P and SBR *vs.* F_N relationships depended, strongly, of the TEE of lines. A complicated behaviour of SBR as a function of TEE lines was observed; when P and F_N were varied. As a result, the selection of unique operating parameter values of P and F_N, for all the studied lines, was impossible. At this point, it was decided to study ME as a function of P, F_N and of TEE of lines before a final selection of the operating parameters.

3.2. Matrix effect study

As known, ME is highly influenced by the operating plasma conditions [22]. At robust plasma operating conditions ME is, generally, reduced; while the opposed effect is observed at non-robust conditions. In order to study the characteristically ME of the matrices considered in this work at robust and no robust plasma, the I MgII 280.270 nm/I MgI 285.213 nm ratio (MgII/MgI) was experimentally determined (Fig. 5) as a function of F_N, from 0.7 to 1.3 L min^{-1}, in a wide interval of P, from 0.9 to 1.5 kW. As expected [13], the most robust plasma (MgII/MgI > 8.2) was obtained for the highest P

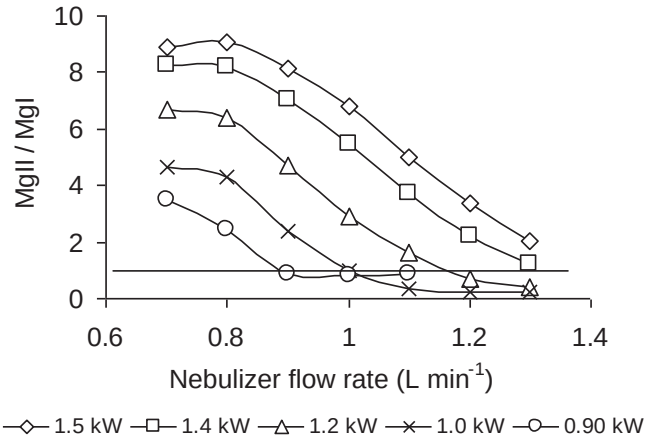

Fig. 5. Radiofrequency power (P) and nebulizer gas flow rate influence on plasma robustness evaluated by MgII/MgI ratio.

(1.4–1.5 kW) and lowest F_N (0.7–0.8 L min^{-1}); whereas the robustness of plasma decreased (MgII/MgI < 1) with the increment of F_N (F_N > 1.0 L min^{-1}) and the reduction of P (P < l.2 kW). The obtained higher and lower MgII/MgI values were similar to those previously measured [8] in a DV 3000 Perking Elmer Spectrometer by using the axial plasma view mode, during the analysis of other ceramic types.

From the practical point of view the selection of the robust conditions previously obtained by evaluating the MgII/MgI ratio seems to be the best choice. However, it is a known fact [11] that, even at robust conditions, the ME can be still significant, principally, for lines with extreme energy excitation. Then, the study of the ME at robust conditions as a function of the TEE of lines is still mandatory for the best selection of analytical lines. On the other hand, in spite of the ICP-OES is a mature analytical technique, from the point of view of the applications, some fundamental aspects related to the excitation mechanisms of lines and to the matrix effect are not still well understood [18–20]. This fact is particularly true for axial view mode ICP-OES, in which the developed fundamental investigations are lesser than similar investigations in radial view observation mode. Thus, the evaluation of ME at no robust conditions and the comparison of ME at robust and no robust conditions could reveal some interesting experimental evidence. Therefore, the ME over the thirty eight analytical lines of thirteen traces was investigated at robust (P = 1.4 kW and F_N = 0.8 L min^{-1}) and no robust (P = 1.2 kW and F_N = 1.3 L min^{-1}) plasma conditions for the three ceramic sample matrices with molar Zr/Ti ratio equal to 20/80 (Fig. 6), 60/40 (Fig. 7) and 80/20 (Fig. 8). The major element concentrations of Pb, Zr, Ti and Sr were 64.38, 5.96, 12.51 and 1.43% for matrix I; 60.93, 16.92, 5.92 and 1.36% for matrix II; and 59.34, 21.97, 2.88 and 1.32% for matrix III.

Generally, the magnitude and sign of the effect varied over a wide range as a function of the TEE of lines and the operating conditions (Figs. 6–8). As expected from other studies in axial [13,20] and radial viewing mode [13], the following ME general characteristics were observed at robust plasma conditions (Figs. 6a–8a) for all the matrices and the most of analytical lines considered. (1) ME was lower than the ME at no robust conditions; (2) ME was closer correlated with the TEE of lines than ME at no robust conditions; (3) The higher ME was achieved for lines with extreme TEEs. Higher signal intensity enhance was observed for lines with TEE of around 2 eV; while higher depression was accounted for lines with TEE around 16 eV. For matrices II and III, the EM *vs.* TEE regression lines crossed the "*x*" axis at TEE ~8 eV. It is the TEE value that divides the lines in "hard" and "soft" types, according to the classification firstly proposed by Boumans [17], later more deeply studied by Kawaguchi

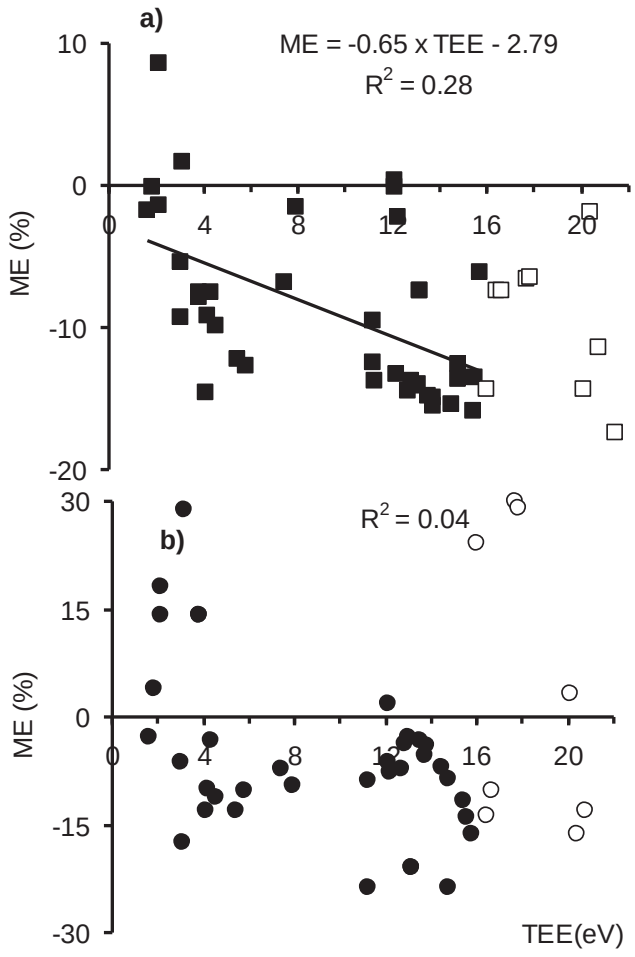

Fig. 6. Variation of the (ME) with the total excitation energy (TEE) of line at: (a) robust (P = 1.4 kW and F_N = 0.8 L min^{-1}), and (b) no robust (P = 1.2 kW and F_N = 1.3 L min^{-1}) conditions for matrix I (Zr/Ti = 20/80).

[22] in radial view mode and also reported by Larrea [20] in axial view mode. Contrastingly, the regression line of EM *vs.* TEE relationship of matrix I was located in the fourth quadrant; where ME was negative (intensity line suppression) for almost lines. On the other hand, some specific characteristics of the ME behaviour, observed in this work at robust conditions (Figs. 6a–8a) for the matrices under study, should be remarked: (1) For all the matrices studied, the correlation between ME and TEE was observed for lines with TEE up to around 15.73 eV, near the first ionization energy (15.76 eV) of Ar atoms. For the remaining lines with TEE in the range of 15.73–21.41 eV, no correlation was observed; (2) In the presence of the matrix I, the ME for all lines was depressive, except for Na 589.592 nm; (3) Correlation coefficient (R^2) of the ME *vs.* TEE relationship was lower for matrix I (R^2 = 0.28), than that for matrices II (R^2 = 0.63) and III (R^2 = 0.68). Nevertheless, the correlation between EM and TEE was still statistically significant for matrix I.

At no robust conditions (Figs. 6b–8b), a higher ME was, generally, observed in comparison with ME at robust conditions; and ME of studied matrices was not correlated to the TEE of line. The no significant correlation coefficients were, 0.04, 0.02 and 0.0006 for matrices I, II and III, respectively. Once more, a particular behaviour was observed in the presence of matrix I: the ME was, generally, depressive for all lines. Contrastingly, the presence of matrix II and III at no robust conditions provoked an increase of I_N for the most of lines considered.

Obviously, the differences in the ME behaviour of the matrix I could be conditioned by his different composition. Note that Ti

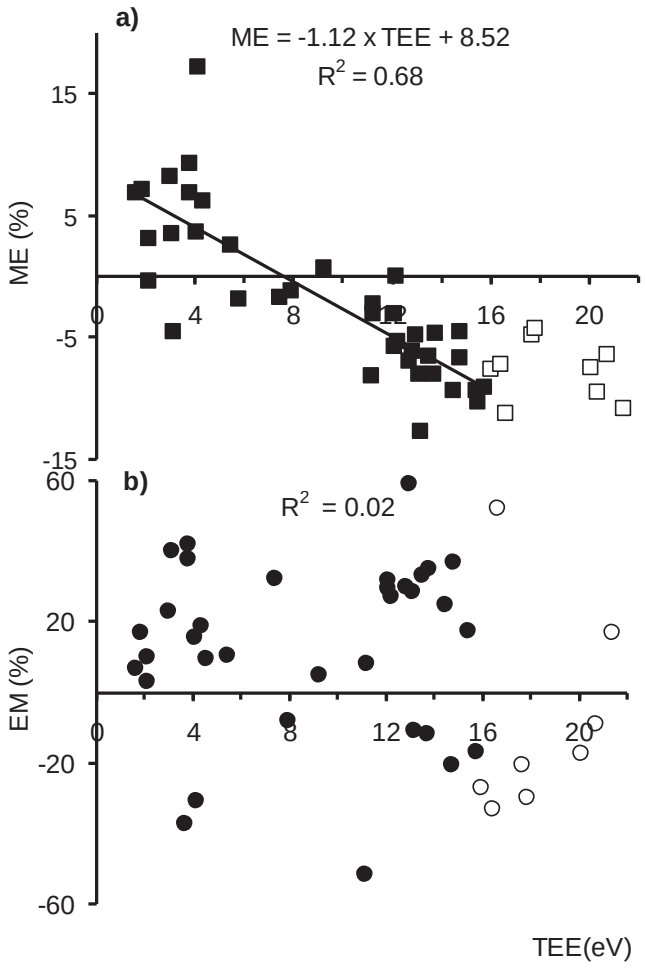

Fig. 7. Variation of the matrix effect (ME) with the total excitation energy (TEE) of line at: (a) robust (P = 1.4 kW and F_N = 0.8 L min^{-1}), and (b) no robust (P = 1.2 kW and F_N = 1.3 L min^{-1}) plasma conditions for matrix II (Zr/Ti = 60/40).

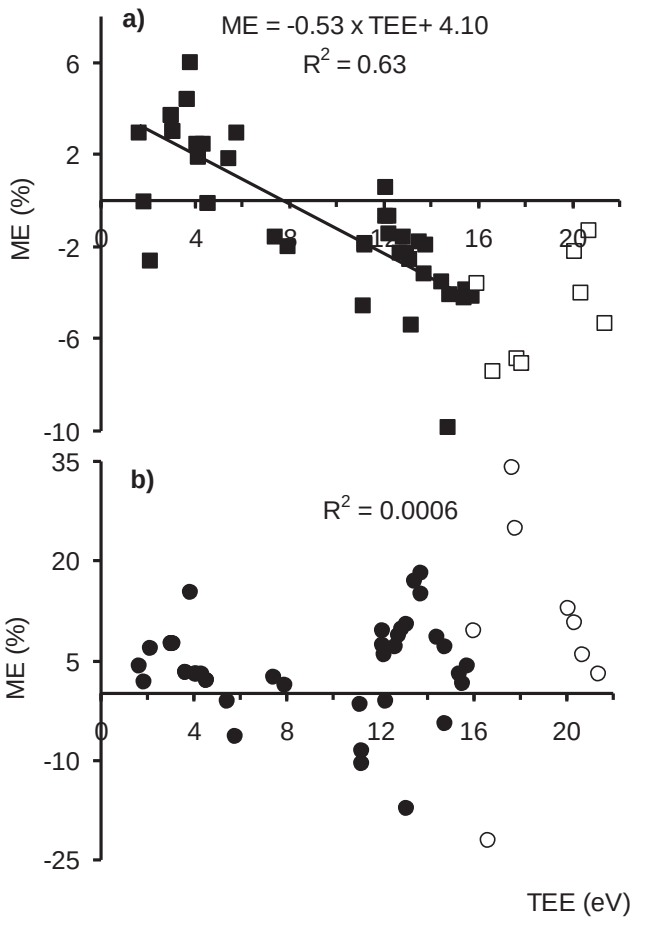

Fig. 8. Variation of the matrix effect (ME) with the total excitation energy (TEE) of line at: (a) robust (P = 1.4 kW and F_N = 0.8 L min^{-1}), and (b) no robust (P = 1.2 kW and F_N = 1.3 L min^{-1}) conditions for matrix III (Zr/Ti = 80/20).

concentration (12.51%) is higher in the matrix I than that of matrices II (5.92%) and III (2.98%); while the lowest Zr concentration (5.96%) is present in matrix I comparing to matrices II (16.92%) and III (21.97%). A detailed investigation for a full explanation of the observed matrix behaviour differences should be conduced, but they were out of the scope of the present work.

3.3. Method parameters and samples analysis

From the practical point of view, the systematic study carried out in this work indicated that the selection of plasma operating robust conditions is the best solution in order to reduce the possible systematic error of the analysis due to matrix effect. In fact, the selected lines, marked in Table 3, showed a minimal ME at

Table 6
Analytic results for ceramic samples at selected nebulizer argon flow rate of 0.8 L min^{-1} and plasma power of 1.4 kW.

Analyte	Added (mg kg^{-1})	Found[a] (mg kg^{-1})	Accuracy (%)	Precision[b] (%)	Limits of detections[c] (mg kg^{-1})	
					Present work	Reported in [9]
Al	10	10.7 ± 0.3	107	5	0.87	12
Ca	4	4 ± 1	100	10	4.45	0.07
Cr	1	0.98 ± 0.09	98	3	0.77	17
Cu	0.5	0.5 ± 0.3	100	13	0.04	3.3
Fe	0.5	0.6 ± 0.1	120	8	10.38	4.6
Mn	1	0.98 ± 0.03	98	12	0.004	2.1
Mg	1	0.97 ± 0.04	97	13	0.04	0.1
Ni	1	0.98 ± 0.04	98	5	0.17	7.9
Zn	0.2	0.2 ± 0.1	100	11	0.06	3.2
Ba	5	5.2 ± 0.5	104	6	0.07	0.3
K	5	5.5 ± 0.7	110	11	5.25	[d]
Co	1	1.02 ± 0.02	102	5	0.03	7.1
In	1	0.92 ± 0.02	92	4	0.1	[d]

[a] Mean concentration ± confidence interval (n = 6, α = 0.05) in mg kg^{-1}.
[b] Evaluated as relative standard deviation of 9 replicates performed.
[c] Evaluated as the limit concentration corresponding to the average concentration of 10 replicates of blank solution plus three times the standard deviation of blank.
[d] No reported.

Table 7
Analysis results (average concentration ± standard deviation, in mg kg^{-1}) for $n = 3$ replicates of some ceramic samples. The analysis was performed at nebulizer argon flow rate of 0.8 L min^{-1} and radiofrequency power of 1.4 kW.

Element	Ceramic molar ratio Cr/Zr/Ti		
	04/60/40	05/80/20	03/53/47
Cr	330 ± 5	368 ± 7	238 ± 20
Ca	231 ± 15	186 ± 28	1292 ± 63
Zn	10 ± 2	2.4 ± 0.5	11 ± 3
Fe	39 ± 3	28 ± 6	29 ± 8
Ba	316 ± 5	354 ± 3	295 ± 7
Mg	9.9 ± 0.6	[a]	[a]
K	92 ± 13	[a]	55 ± 4
Co	81 ± 2	34.6 ± 0.5	73 ± 10
In	365 ± 10	640 ± 11	362 ± 16
Al	1076 ± 13	1326 ± 76	912 ± 49

[a] Concentrations below the LODs. Cu, Ni and Mn, were below LODs in all analyzed samples.

those conditions. For instance, ME of Fe 259.941 nm, K 766.491 nm and Co 228,616 nm was 6, 7 and 8%, respectively. Nevertheless, it should be noted that SBR of some lines at robust conditions could be lower than that at no robust conditions. In a first approximation, we decided prioritizing the improvement of accuracy by selecting the plasma operating robust conditions. Then, method performance parameters were evaluated at $P = 1.4$ kW and $F_N = 0.8$ L min^{-1}.

The limits of detections, precision and accuracy of the developed method are shown in Table 6. LODs of Cr and impurities Al, Ca, Cu, Cr, Fe, Mn, Mg, Ni, Zn, Ba, K, In and Co, were calculated in the presence of the Zr/Ti = 60/40 matrix sample, taken as example of the investigated ceramics. LODs were between 0.004 μg g^{-1} for Mn up to 10 μg g^{-1} for Fe; and they were, generally, better than those reported for the same elements determined in Nb doped PZTs ceramic [9]. The precision, given as relative standard deviation (RSD), varied between 3% for Cr and 13% for Cu. The analytes recoveries in the spiked ranged from 90 to 110%, excepting Fe (120%). In virtue of the quantitative analyte recovery, which was guaranteed at the robust plasma conditions employed, the investigated elements could be determined by means of external calibration, using calibration solutions prepared with HNO_3 only.

The analysis results of three ceramic samples with different major element composition are shown in Table 7. Mn, Cu and Ni concentrations were below the LODs in all samples. Interestingly, the content of Fe (~34 mg kg^{-1}) and Ba (~320 mg kg^{-1}) were similar for all samples. The lower content of Zn, K and Co in the 05/80/20 ceramic appears to be associated with the lower amount of Ti; while the higher content of In and Al in the same ceramic could be related with the higher amount of Zr in this ceramic. In both cases, the impurities could be provided by the reagents employed in the ceramic synthesis process. The PZTs ceramics substituted by Sr and Cr, analyzed in the present work, showed contents of Ba, Zn and Al similar to those contents found in doped Nb PZTs ceramics [9]. In contrast, Fe and Mg were higher and Ca and Co was lower in the Nb doped ceramics than in ceramics of the actual study.

4. Conclusions

During the optimization of the analytical procedure some interesting results were pointed out:

- The highest sensitivity of the I_N with P and F_N variations was observed for ionic lines with TEE in the range of 9.06–12.19 eV. It should be remarked that the behaviour of I_N with P and N_F variation observed for this particular group of lines has not been so far reported in axial view mode. In our opinion, this coincidence was not casual and, the observed experimental results could be explained by an over excitation of the trace excitation energy levels by Penning Reaction. However, the confirmation or refutation of this hypothesis need for a more exhaustive investigation, which was out of the scope of the present work.
- For all the matrices and the most of analytical lines considered, the ME at robust plasma conditions was, as expected; lower than the ME at no robust conditions and, also ME close correlated with the TEE of lines. The higher MEs were, generally, achieved for lines with extreme TEEs. A particular behaviour of ME in the presence of matrix I (Zr/Ti = 80/20) with a higher concentration of Ti was observed. In this matrix the ME was, generally, depressive for all lines.
- As a result of the systematic investigation developed, an assisted-microwave acid digestion procedure and a further axial observation mode inductively coupled plasma optical emission spectrometry quantification method was obtained for the determination of the doped Cr and the impurities Al, Ca, Cu, Fe, Mn, Mg, Ni, Zn, Ba, K, In and Co in lead zirconate-titanate ceramics, modified with strontium and chromium. The precision of analysis ranged from 2.5 to 13%, whereas the analytes recoveries in the spiked samples varied, mostly, from 90 to 110%, excepting Ca (115%). The detection limits of studied elements were from 0.004 to 10 mg kg^{-1}.

Acknowledgements

This work has been performed in the frame of the International Cooperation Program of the Universidad Complutense de Madrid with La Universidad de la Habana and the IMRE Project "Confidence improvement of the environmental samples and advanced materials analyses" of the 2011 convocation.

References

[1] B. Jaffe, W.R. Cook, H. Jaffe, Piezoelectric Ceramics, vol. 362, Academic Press, New York, 1971.
[2] L.E. Cross, Ferroelectric Ceramics: Tailoring Properties for Specific Applications, Birkhäuser Verlag, Basel, London, 1993.
[3] R. Sitko, B. Zawisza, A. Kita, M. Plonska, Anal. Bioanal. Chem. 385 (2006) 971.
[4] J. de los Santos Guerra, P. Barranco, F. Calderón, D. Garcia, J.A. Eiras, Cerâmica 51 (2005) 19.
[5] J. Costa, A. Suárez, J. Saniger, F. Calderón, Rev. Cub. Física 26 (2A) (2009) 174.
[6] J.C. Fariñas, M.F. Barba, J. Anal. At. Spectrom. 7 (1992) 869.
[7] A. Montaser, D.W. Golightly, Inductively Coupled Plasmas in Analytical Atomic Spectrometry, VCH, New York, 1987.
[8] Y. Mosqueda, M. Pomares, E.L. Pérez-Cappe, A. Miranda, J.C. Fariñas, M.T. Larrea, Anal. Bioanal. Chem. 386 (2006) 1855.
[9] J.C. Fariñas, M.F. Barba, J. Anal. At. Spectrom. 7 (1992) 877.
[10] L. Paama, E. Parnoja, P. Peramaki, J. Anal. At. Spectrom. 15 (2000) 571.
[11] I.B. Brenner, A.T. Zander, Spectrochim. Acta B 55 (2000) 1195.
[12] L.C. Trevizan, J.A. Nȍbrega, J. Braz. Chem. Soc. 14 (2) (2003) 310.
[13] J.L. Todolí, L. Gras, V. Hernandis, J. Mora, J. Anal. At. Spectrom. 17 (2002) 142.
[14] J.M. Mermet, J. Anal. At. Spectrom. 20 (2005) 11.
[15] M.T. Larrea, I. Gómez-Pinilla, J.C. Fariñas, J. Anal. At. Spectrom. 12 (1997) 1323.
[16] M. Villanueva-Tagle, D. Pozebon, R. Hernández, F. Calderón, M.D. Durruthy, M. Pomares, Spectrosc. Lett. 44 (2011) 138.
[17] P.W.J.M. Boumans, F.J. De Boer, Spectrochim. Acta B 32 (1977) 365.
[18] C. George, Y. Chan, G.M. Hieftje, Spectrochim. Acta B 61 (2006) 642.
[19] G.C.-Y. Chan, G.M. Hieftje, Spectrochim. Acta B 59 (2004) 1007.
[20] M.T. Larrea, B. Zaldıvar, Juan C. Fariñas, L.G. Firgaira, M. Pomares, J. Anal. At. Spectrom. 23 (2008) 145.
[21] J.M. Mermet, Anal. Chim. Acta 250 (1991) 85.
[22] H. Kawaguchi, T. Ito, K. Ota, A. Mizuike, Spectrochim. Acta B 35 (1980) 199.